

A NEW LOW NOISE, HIGH GAIN ANTENNA

S. R. Jones and K. S. Kelleher

Aero Geo Astro Corporation
Alexandria, Virginia

Reprinted from:

1963 IEEE INTERNATIONAL CONVENTION RECORD
Part 1

A NEW LOW NOISE, HIGH GAIN ANTENNA

S. R. Jones and K. S. Kelleher
Aero Geo Astro Corporation
Alexandria, Virginia

A new antenna type is described which combines the low noise temperature characteristics of the horn-reflector antenna with the more attractive mechanical features associated with the paraboloidal reflector. Cassegrain optics used in an off-set feed configuration enables a virtual source to be formed without sub-reflector blockage. An extremely compact structure is realized with a concave hyperboloid which mirrors the actual feed located on the paraboloidal surface. Except for the aperture, the antenna is completely shielded. The design approach is outlined and measurements on an experimental model are presented. Ground noise contribution from minor lobes is about 2°K.

Introduction

Ultimate sensitivity of many present day receiving systems is determined by the antenna temperature rather than the receiver noise figure. Noise temperature and noise figure are related by $T = (NF - 1)T_0$; T_0 is a reference temperature usually taken to be 290°K. With reference to other writers we shall simply state that the effective antenna noise temperature is a function of antenna gain and the spatial distribution of thermal sources.¹ More precisely,

$$T_A = \frac{1}{4\pi} \int_{\Omega} G(\theta, \phi) T(\theta, \phi) d\Omega$$

where $d\Omega = \sin \theta d\theta d\phi$, the element of solid angle. Gain and temperature are specified in terms of polar coordinates and the integration is performed over all space.

For our purposes, the distribution of thermal noise sources can be considered almost independent of the azimuth angle. The variation with frequency is indicated in Figure 1 for several elevation angles. A reasonably low noise temperature over a wide range of frequencies is suggested by this figure for an antenna admitting no side or back lobes and pointed at elevation angles higher than 10 degrees. Atmospheric absorption causes a sharp increase in this level at lower angles and finally, the noise temperature of the earth is nominally 240°K for a typical emissivity of 0.85. From this distribution and the above equation, it is apparent that a zenith oriented narrow beam antenna operating at, say 2 Gc, could have a noise temperature ranging from less than 5 degrees to greater than 100°K depending upon its average backlobe level; this

backlobe component of noise temperature is graphed in Figure 2. In many antennas this level is largely determined by feed spillover.

Because signal-to-noise ratio is the factor indicating system performance, it is clear that aperture efficiency is also of paramount importance.² A reduction in antenna temperature with a concomitant reduction in gain is usually of little practical interest since this leaves the ratio unchanged. Using this criterion, the comparative performance of three reflector type antennas is next outlined.

Feed spillover is the most serious disadvantage of focal point fed paraboloids because this is directed at the earth for even moderately high elevation pointing angles. Figure 3-a illustrates this schematically. A compromise between under illumination of the reflector and relatively high spillover is always required with a $(\cosine)^n$ type primary pattern; optimum gain is realized with an edge illumination on the order of -10 db for most reflector shapes. Shaped primary feed patterns providing almost uniform aperture illumination with a sharp reduction in spillover energy have however, improved this situation.^{2,3} Transmission line losses in the feed system are not treated in this paper but it may be noted that a practical system requires the preamplifier to be situated at the focal point in order to minimize this source of noise.

A conventional Cassegrain antenna is sketched in Figure 3-b. Here, feed spillover past the sub-reflector is usually directed into a relatively cool region of the sky. Consequently, its effect on antenna noise is not so severe as with the focal point feed system. Also, the preamplifier can be mounted conveniently on the rear of the reflector in close proximity to the primary feed. Aperture blocking by the sub-reflector does, nevertheless, restrict recommended use of this system to requirements for half power beamwidths not greater than 2 degrees.

Another antenna type used in space communications is the horn-reflector shown in Figure 3-c. Several of its electrical advantages are apparent. First, the metallic horn flares prevent spillover from the feed so an extremely low antenna temperature is possible. Second, the off-set feed avoids aperture blocking and reasonably high aperture efficiencies can be realized.

From an R-F standpoint the horn-reflector then seems a most attractive choice. Its mechanical features, however, are frequently not as satisfying as those of the paraboloid. The relatively long horn throat necessitates a large and awkward size for the entire structure compared with the useful aperture. An application of Cassegrain optics described next has eliminated the horn throat and retained the R-F characteristics of the horn reflector.

Development of the Design

The Cassegrain configuration is derived from the horn-reflector type antenna shown in Figure 4. A parabolic curve with vertex at the origin and focal length $f = OF$ (Figure 4-a) is given by $y^2 = 4fx$. Rays emerging from the point F are collimated upon reflection from any section of the parabola. For our purposes, this curve is more usefully expressed in terms of r , the radius vector drawn from F to the curve, and α , the angle of this vector from the line FF' . Counterclockwise angles are taken as positive and FF' is perpendicular to OF for reasons of aperture blocking which will later become more apparent. In terms of these parameters, the parabolic section is written,

$$r = \frac{2f}{1 + \sin \alpha}, \quad +\alpha_0 \leq \alpha \leq -\alpha_0 \quad (1)$$

$+\alpha_0$ and $-\alpha_0$ define the section of this parabola forming the horn-reflector. Three conditions are of special interest: $r = r_1$, when $\alpha = +\alpha_0$; $r = r_2$ when $\alpha = -\alpha_0$; and $r = FF'$ when $\alpha = 0$. From Equation (1):

$$r_1 = \frac{2f}{1 + \sin \alpha_0} \quad (2)$$

$$r_2 = \frac{2f}{1 - \sin \alpha_0} \quad (3)$$

$$\text{and, } FF' = 2f \quad (4)$$

Rotation of the parabolic section about the OX axis generates the parabolic surface. Figure 4-b is a front view for a symmetrical rotation angle, α_0 .

Conventionally, the horn-reflector appears in the form of Figure 4 with metal flares guiding waves from the feed point, F , until they emerge as a parallel beam at the aperture, D . Now, from Figure 4, $D = y_2 - y_1$ where $y_1 = r_1 \cos(+\alpha_0)$ and $y_2 = r_2 \cos(-\alpha_0)$. With appropriate substitutions, this becomes,

$$D = 4f \tan \alpha_0 \quad (5)$$

The focal length of the paraboloid from which the reflector may be imagined to be taken, and

the horn flare angle thus define the aperture dimension of the horn-reflector.

The new design employs Cassegrain optics to form a virtual source at the focal point of the paraboloidal section, F , when the actual feed is situated at F' . A concave hyperbola with foci at F and F' is defined in Figure 5 by

$$\xi - \rho = 2a. \quad (6)$$

Also, from the figure,

$$\xi = \left[(\rho \sin \psi)^2 + (2f - \rho \cos \psi)^2 \right]^{1/2}$$

which substituted in Equation (6) yields,

$$\rho = \frac{f^2 - a^2}{a + f \cos \psi} \quad (7)$$

Equation (7) represents a family of curves satisfying our focusing requirement. In order to define the surface for our design we must specify "a", which is in turn dependent upon the maximum angle intercepted by the hyperbola, ψ_0 . The angle $2\psi_0$ is the actual feed angle. This consideration, as well as a desire to realize a relatively short overall length, dictates an hyperbola intercepting the parabolic section at the point normally made by the horn of flare angle α_0 . This is sketched in Figure 6; from this figure we may write,

$$\tan \psi_0 = \frac{r_1 \sin \alpha_0}{2f - r_1 \cos \alpha_0} \quad (8)$$

Substituting the value of r_1 given by Equation (2),

$$\psi_0 = \tan^{-1} \left[\frac{\sin \alpha_0}{1 + \sin \alpha_0 - \cos \alpha_0} \right] \quad (9)$$

At $\psi = \psi_0$, Equation (6) becomes,

$$2a = r_1 - \rho_1 \quad (10)$$

Where r_1 is given by (2) and from the geometry of Figure 6,

$$\rho_1 = \frac{r_1 \sin \alpha_0}{\sin \psi_0} \quad (11)$$

Substitution of Equations (2) and (11) in (10) yields,

$$a = \frac{f(\sin \psi_0 - \sin \alpha_0)}{\sin \psi_0 (1 + \sin \alpha_0)} \quad (12)$$

with ψ_0 given in (9) as a function of α_0 . The desired hyperboloid is generated by rotation about FF' of the hyperbolic section

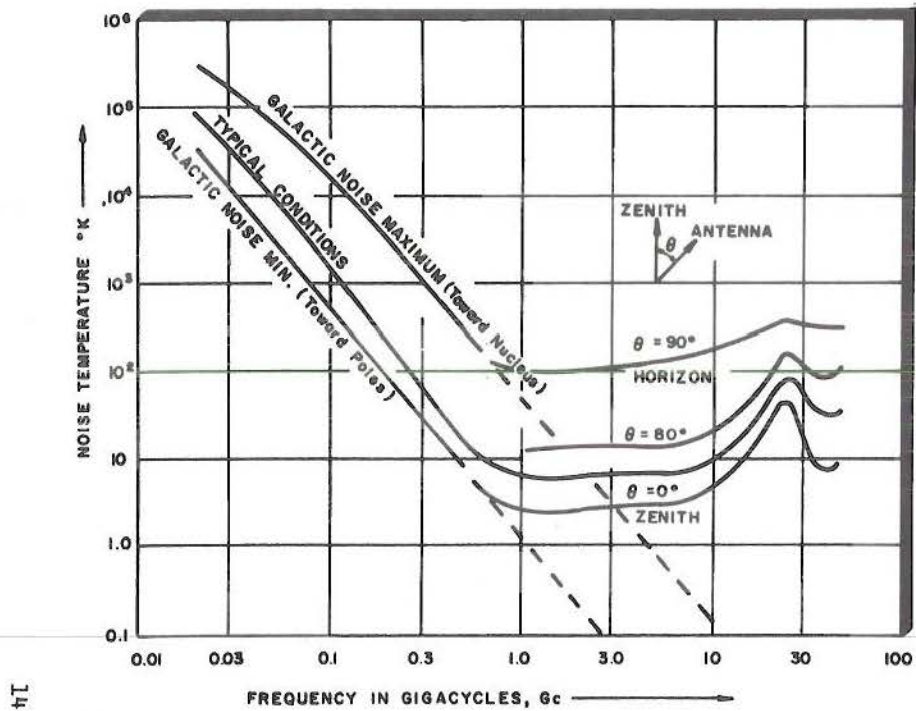


Fig. 1. Summary Plot of Environmental Noise Temperature Characteristics.

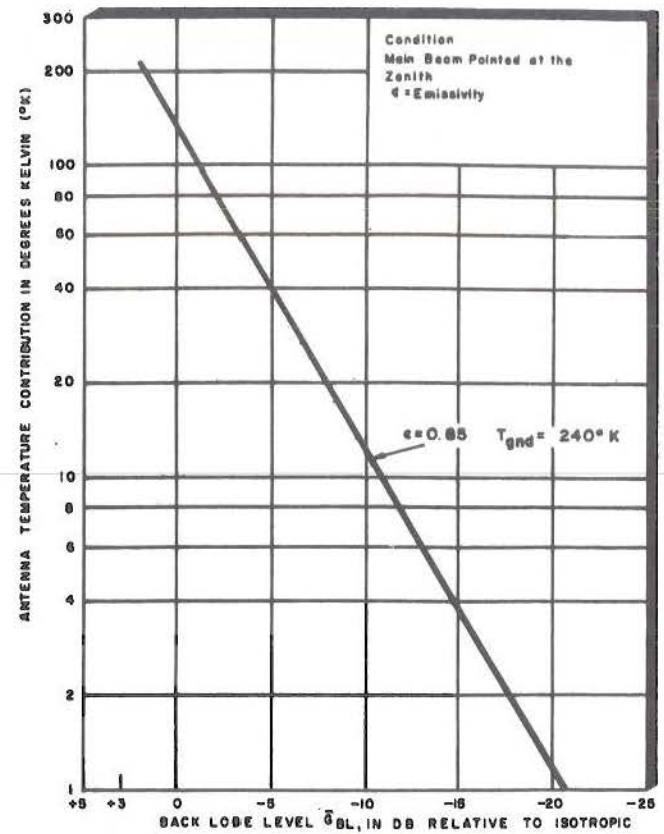


Fig. 2. Antenna Noise Temperature Contributions Calculated from Average Backlobe Level (G_{PL}).

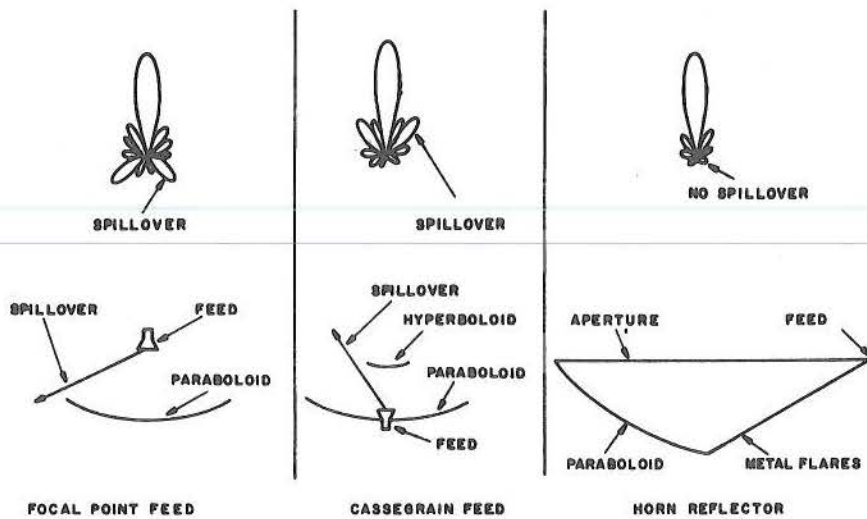


Fig. 3. Spillover for Several Antenna Types.

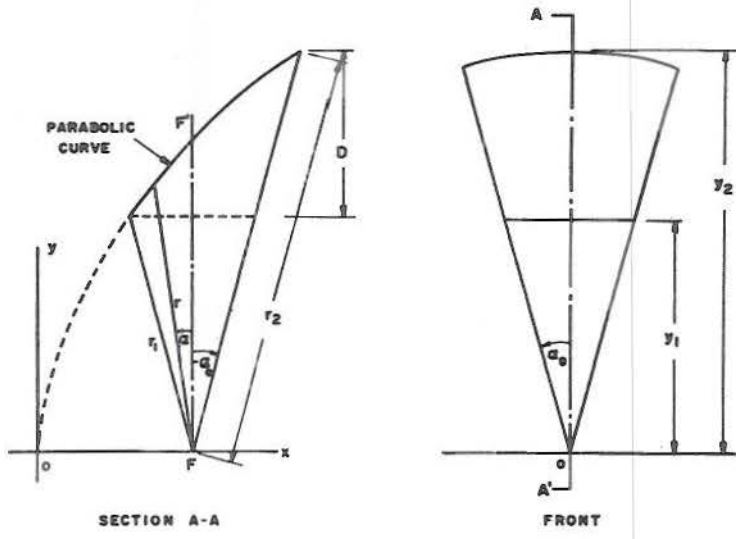


Fig. 4. Horn-reflector Geometry (Side and Front Views).

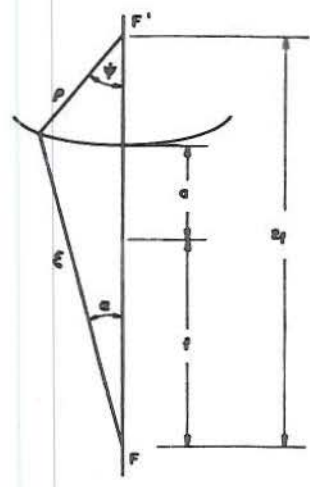


Fig. 5. Hyperbola Geometry.

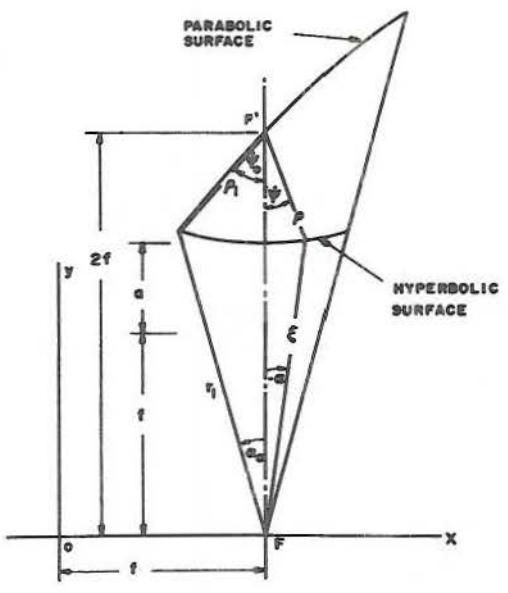


Fig. 6. Evolution of Cassegrain Horn-Reflector.

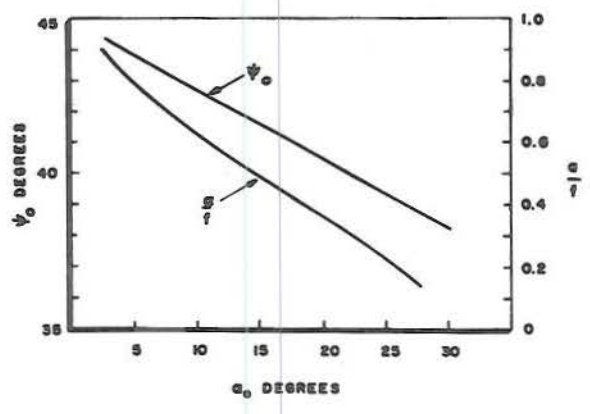


Fig. 7. Design Parameter Relationships.

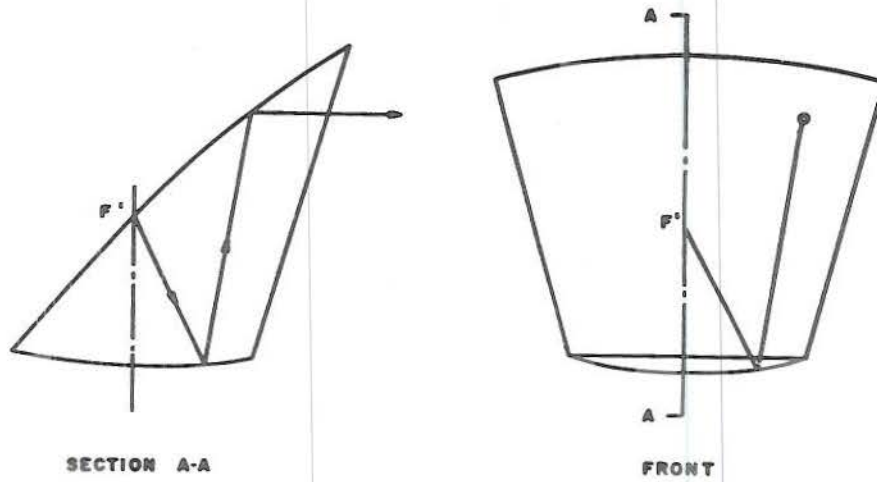


Fig. 8. Typical Ray (Side and Front Views).

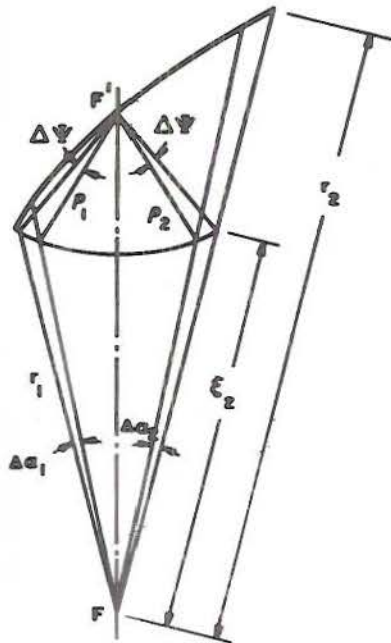


Fig. 9. Geometry for Space Attenuation.

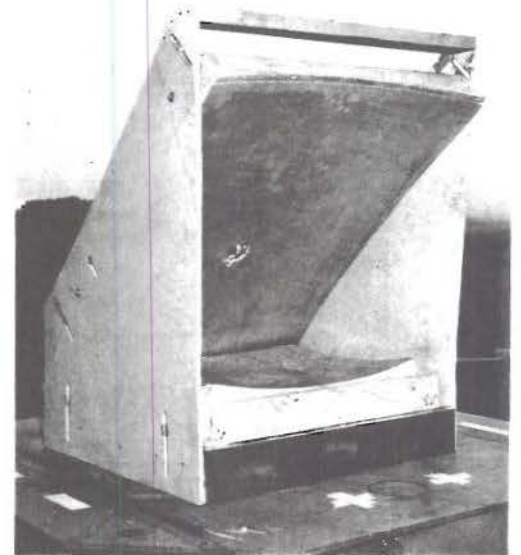


Fig. 10. Experimental Model.

Fig. 11.
Azimuth
Plane
Pattern
(F = 11 Gc)

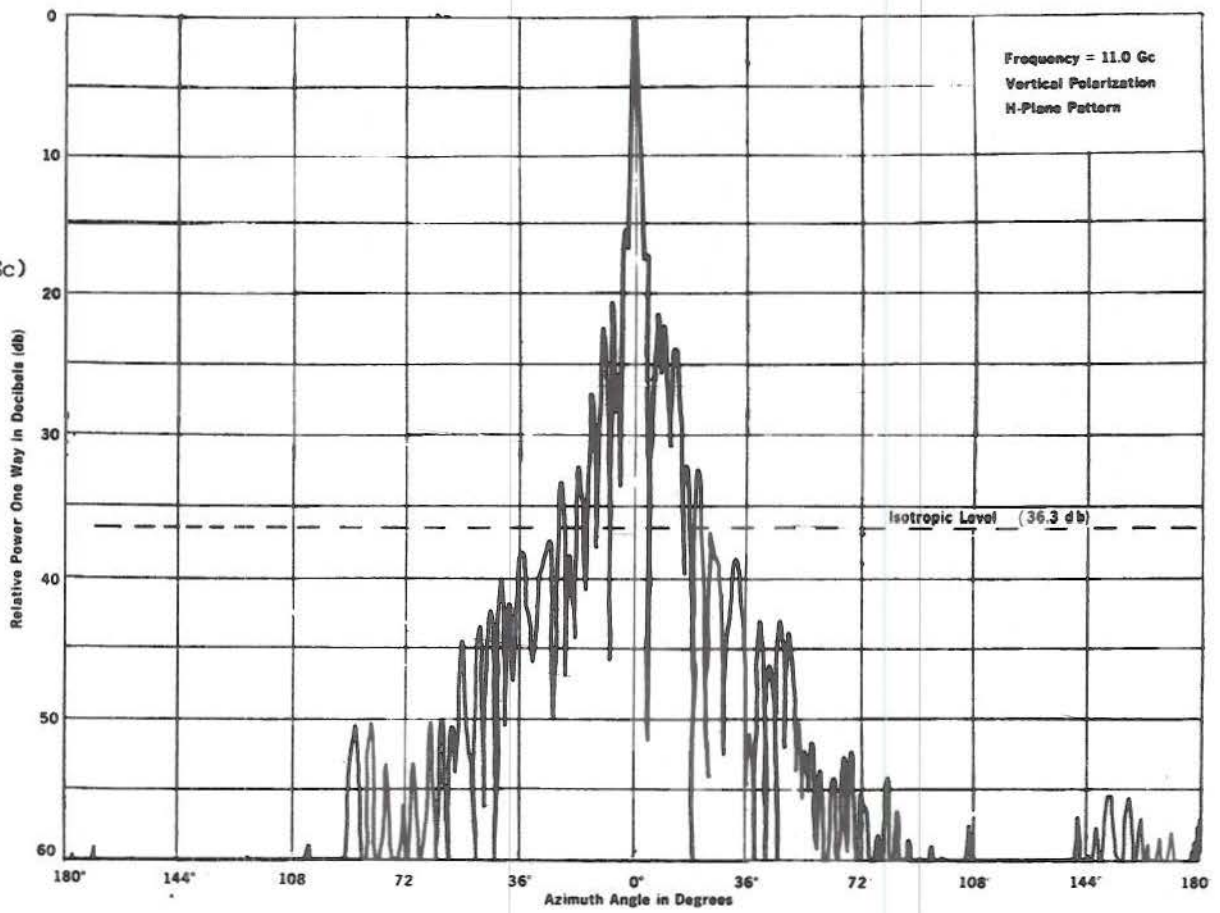


Fig. 12.
Elevation
Plane
Pattern
(F = 11 Gc)

